NASA-TM-109,108

NASA Technical Memorandum 109108

NASA-TM-109108 19940028433

Comparison of the Compressive Strengths for Stitched and Toughened Composite Systems

James R. Reeder
Langley Research Center, Hampton, Virginia

April 1994

National Aeronautics and
Space Administration
Langley Research Center
Hampton, Virginia 23681-0001

ABSTRACT

The compression strength of a stitched and a toughened matrix graphite/epoxy composite was determined and compared to a baseline unstitched untoughened composite. Two different layups with a variety of test lengths were tested under both ambient and hot/wet conditions. No significant difference in strength was seen for the different materials when the gage lengths of the specimens were long enough to lead to a buckling failure. For shorter specimens, a 30% reduction in strength from the baseline was seen due to stitching for both a 48-ply quasi-isotropic and a $(0/45/0/-45/90/-45/0/45/0)_S$ laminate. Analysis of the results suggested that the decrease in strength was due to increased fiber misalignment due to the stitches. An observed increasing strength with decreasing gage length, which was seen for all materials, was explained with a size effect model. The model assumed a random distribution of flaws (misaligned fibers). The toughened material showed a small increase in strength over the baseline material for both laminates presumably due to the compensating effects of a more compliant matrix and straighter fibers in the toughened material. The hot/wet strength of the stitched and baseline material fell 30% below their ambient strengths for shorter, non-buckling specimen, while the strength of the toughened matrix material only fell 20%. Video images of the failing specimen were recorded and showed local failures prior to global collapse of the specimen. These images support the theory of a random distribution of flaws controlling composite failure. Failed specimen appearance however, seems to be a misleading indication of the cause of failure.

INTRODUCTION

Composite materials are now being considered more often for primary structures. As composite structures compete with metal structures there is pressure to make composites faster, cheaper, and stronger. The in-plane properties compare very well with metals. However, low out-of-plane properties of composite materials have lead to delamination problems and low damage resistance. Two methods can be used to improve these thickness-direction properties: the matrix can be toughened; or through-the-thickness fiber arrangements can be employed. Tougher matrix systems have shown dramatic improvements in damage resistance [1] as has through-thickness stitching [2]. Of course, changing the matrix properties or introducing stitches to a laminate will affect the in-plane properties, and aircraft structures are primarily sized by in-plane properties. The objective of this work was to determine the influence of stitching versus a toughened matrix on the in-plane compression strength of composite materials.

First, the compression failure of an unstitched material made of AS4/3501-6 was studied to provide a baseline. This material was then compared to both a stitched composite made of the same fiber and matrix and to an unstitched composite made of the same fiber but with a tough matrix (8551-7 epoxy). Analyses were developed to model the compression strength of the baseline material. These models were then used to explain the differences observed in compression strength between the baseline and both the stitched and the toughened matrix materials.

Several factors which can affect the compression response of a laminate were investigated. First, because laminate compression strength is a complex combination of material and structural response, tests over a wide range of unsupported specimen gage lengths were conducted. Second, since composite laminates are tailored to different applications, laminates which differed in stacking sequence and thickness were tested. Compression results of a moderately thick common quasi-isotropic laminate were studied and then compared to a thinner $(0/45/0/-45/90/-45/0/45/0)_s$ laminate, which was stronger and stiffer in the 0° direction. The final factor studied was the effect of environment. Initially all the laminates were tested at room temperature and under ambient moisture conditions. Tests were then run at 180°F on specimens which had been subjected to a prolonged water soak. Such hot/wet properties are often used in design because they represent one of the more critical environments that a normal aircraft structure might be expected to endure.

SYMBOLS LIST

A	cross-sectional area of specimen, in^2
C	end constraint coefficient
E	laminate longitudinal modulus, Msi
G	laminate through-thickness shear modulus, Msi
G_m	matrix tangent shear modulus, Msi
I	bending moment of inertia, in^4
L	specimen gage length, in
m	Weibull slope parameter
t	specimen thickness, in
V_f	fiber volume fraction
V_m	matrix volume fraction
w	specimen width, in
α	initial fiber misalignment, rad.
β	rotational spring stiffness, in-lb/rad
γ	composite shear strain

γ_m	matrix shear strain
σ	laminate strength, ksi
σ^o	strength in 0° ply, ksi
$\sigma_{0.5}$	reference laminate strength at 0.5 in. gage length, ksi
$\sigma^o_{0.5}$	0° ply strength at reference 0.5 in. gage length, ksi
τ_m	shear stress in matrix, ksi

MATERIAL

Traditionally, composite material has been manufactured by stacking together layers of prepreg tape material. Prepreg tape is a combination of unidirectional fibers and partially cured matrix. These layers are then consolidated by heating them under pressure to form a laminate. Unfortunately, when these layers of prepreg are stitched, some fibers are broken because they are held in place by the partially cured matrix. These broken fibers significantly reduce the in-plane properties of the composite [3]. To solve this problem, stitched laminates have more recently been made from uniweave fabric. The uniweave fabric material does not contain the partially cured matrix, so fibers are able to move out of the way of the needle and thus fewer fibers are broken [3]. In the uniweave layer, a small percentage of thin compliant glass fibers are woven transverse to the aligned fibers to hold the layer together so it can be handled. Once a stack of uniweave layers has been stitched, it is put into a mold and low viscosity resin is heated and forced to infiltrate the laminate. This process is called resin transfer molding (RTM). The mold is then heated to cure the matrix.

The baseline material in this study was an uniweave laminate without stitching. The base line laminates were manufactured with the RTM process used for the stitched laminates. The uniweave material was made of AS4 fibers in the primary direction. The weaving fibers were glass and only accounted for 1% of the fabric weight. The matrix was 3501-6 epoxy which is a common low-toughness composite matrix. The stitched laminates consisted of uniweave plies stitched with a 1250 yd/lb glass yarn. The laminates were stitched in the load carrying direction with eight rows of stitches per inch. Within a row, a stitch was made every 1/8 of an inch using a modified lock stitch. This stitch placed the stitch knot on the back surface of the laminate where it would have less of an effect on the fibers in the laminate [2]. The toughened matrix material was a conventional prepreg tape. The prepreg tape contained the same AS4 fibers as in the baseline and stitched materials, but had a toughened 8551-7 epoxy matrix. These laminates were manufactured in an autoclave curing process.

Two laminates of each material were tested. The first was a 48-ply quasi-isotropic laminate with a $(45/0/-45/90)_{6S}$ layup which was intended to represent an aircraft frame structure. The laminate thickness, t, was approximately 0.25 inches. The other laminate was a 0.1 in. thick 18-ply $(0/45/0/-45/90/-45/0/45/0)_S$ laminate. This laminate was stiffer and stronger than the quasi-isotropic laminate because of the larger proportion of 0° plies and represented a wing skin.

TESTS SPECIMEN AND PROCEDURE

The compression tests in this study were conducted using a NASA linear-bearing fixture [4] as shown in Figure 1. This fixture has four rods mounted with linear bearings to keep the grips aligned. The test specimen extended 2.25 in. into each grip, load was introduced primarily through end loading. The face grips primarily provided lateral restraint. They also reduced the tendency for the specimen to fail at the ends by introducing some of the load through shear thereby reducing the end loads. Soft plastic shims were placed between the grips and the specimen so that the grip faces did not bite into the test specimen and so that the stress concentration at the grip line was reduced. This loading configuration did not require the use of bonded tabs. Bonded tabs, which are required for many other compression tests [5], have been shown to cause a significant stress concentration at the end of the gage section [6, 7] as well as requiring an additional manufacturing step. This fixture was modified slightly from that described in Reference 4, to allow laminates of different thicknesses to be tested. The back grip plate was made adjustable so that the centerline of the test specimen could be aligned with the centerline of the load frame.

All test specimens had a 1 in. width, w, but ranged in length between 4.69 and 14.5 inches. These specimens had unsupported gage lengths, L, of 0.19, 0.5, 1.0, 2.0, 3.5, 5.5, and 10.0 inches. Only the thicker quasi-isotropic laminates were tested with the 5.5 and 10 inch gage lengths. Strain gages were applied to many of the specimens to check specimen alignment, to confirm Euler buckling, to measure longitudinal modulus and Poisson's ratio, and to determine strain at failure. The specimens with 1.0, 2.0, 3.5, or 5.5 in. gage lengths were strain gaged front and back with 1/4 in. strain gages in both the longitudinal and transverse directions. Because of their small gage length, specimens with the 0.5 in. gage length were strain gaged front and back with 3/16 in. strain gages in the longitudinal direction only. The 0.19 in. gage length specimens were too small for strain gage measurements.

As mentioned, compression tests were first run under ambient conditions. The laboratory temperature was 77°F. All ambient specimens contained a nominal amount of moisture since they had been stored under normal atmospheric conditions for a prolonged period.

The hot/wet specimens were soaked in water at 160°F for 45 days and then tested at 180°F. These hot/wet test parameters are similar to those used for general material evaluations [8]. In order to determine the amount of moisture absorbed by the specimen, they were weighed after being dried and again after being soaked. The specimens were stored in water until they were tested. For strain gauging, the specimens were removed from the water for approximately 6 hours while the strain gages were bonded. M-Bond GA-2@ [9] room-temperature-cure epoxy adhesive was used because it provided adequate adhesion under this hot/wet environment. After bonding, the specimens were returned to water for 1 to 2 days before being tested.

To perform elevated temperature tests, an oven was placed around the linear-bearing fixture and heated to 180°F. Prior to testing, each specimen was put in a small water bath which was then placed in the oven. When the water temperature reached 180°F, the specimen was removed from the bath and the excess surface moisture was dried. If the specimen was strain gaged, the specimen was allowed to sit in the oven without being gripped for several minutes until the specimen temperature and strains stabilized so that the gages could be zeroed. The specimen was then placed in the grips and loaded to failure. The specimen was placed in the grips as quickly as possible to minimize drying. The elapsed time between removing the specimen from the 180°F water bath and actually testing was usually less than 30 minutes.

All compression tests were conducted in displacement control. The initial displacement rate was 0.02 in/min but the rate was slowed to 0.01 in/min near failure to better capture the failure mechanisms. The load and crosshead displacement as well as strain readings were recorded every 0.5 seconds. To determine longitudinal modulus, the front and back strain gage readings were averaged and plotted versus load. The modulus was calculated from the slope of a least squares regression line which was fit to the points which fell between 1000 and 3000 $\mu\varepsilon$. The Poisson's ratio was determined by plotting the averaged front and back transverse strain versus the average longitudinal strain. Poisson's ratio was taken as slope of the regression line fit to the points with average longitudinal strains between 1000 and 3000 $\mu\varepsilon$. The front to back longitudinal strain differed by less than 200 $\mu\varepsilon$ when the average longitudinal strain was 3000 $\mu\varepsilon$, indicating that the specimen was well aligned. At least three repetitions of each strength test were performed.

During several of the ambient tests, the machined edge of the specimen was viewed with a high speed video system which recorded 1000 frames per sec. The hot/wet tests were not recorded on video because the oven blocked the edge view of the specimen.

BASELINE MATERIAL AND MODELS DEVELOPMENT

The compression strength of the baseline unstitched uniweave quasi-isotropic laminate is shown in Figure 2. The strength of this material varies widely over the gage lengths tested. This is not surprising since the longer specimens were quite long compared to their thickness and, therefore, buckled. Once the gage length was small enough to prevent buckling one might expect to find some constant "material compression strength" [10]. Instead the compression strength was found to continue to increase as the gage length was reduced. Buckling theory was used to model the longer gage length specimen. The strength in the short gage length region was modeled with a size effect model which will be described later.

The Euler buckling strength a beam with fixed ends is given by

$$\sigma = \frac{4\pi^2 EI}{A2L^2} \tag{1}$$

where I is the bending moment of inertia ($I = w\,t^3/12$), A is the cross-sectional area ($A = w\,t$) and E is the laminate longitudinal modulus. This equation also assumes a homogeneous material. For the laminates in this study which contain dispersed 0, ±45, and 90 degree layers, this assumption should be acceptable. This model used a value of E of 7.18 Msi and an average thickness of 0.255 inches which were measured for these laminates. As can be seen form Figure 2 this model does a poor job of modeling the compression response of the test specimen. Two reasons for this are that it neglects the effect of shear deformation and that it assumes perfectly fixed end conditions. Shear deformation is generally more significant for graphite/epoxy composite beams than for metal beams because the shear modulus is smaller compared to the longitudinal modulus for the composites. Even though a specimen was firmly clamped in each grip, the end condition is not perfectly clamped. The material which was held in the grip was constrained from lateral movement but could deform longitudinally. A gradient in longitudinal deformation across the thickness of the specimen would result in a rotation of the specimen cross section at the grip [11].

Equation 2 [12] accounts for shear deformation and compliance of the end condition.

$$\sigma = \frac{C\pi^2 EI}{A2L^2}\left(\frac{1}{1+1.2\frac{C\pi^2 EI}{A2L^2 G}}\right) \qquad (2)$$

G is the through-the-thickness shear stiffness of the material. The end constraint coefficient, C, for a column which is constrained from lateral movement at the ends and where rotation is resisted by rotational springs is approximated in Reference [13] as

$$C = \frac{\left(EI/\beta L + .4\right)^2}{\left(EI/\beta L + .2\right)^2} \qquad (3)$$

where β is the rotational spring stiffness.

This buckling model is plotted in Figure 2 and agrees well with the strength data at longer gage lengths. The value of G used in the model was 0.691 Msi which was calculated using laminate property transformations described in Reference 14 and the lamina properties given in Table 1. The rotational spring stiffness, β, was chosen to be 16,000 in-lb/rad which produced a good fit to the data. The model does a good job of modeling strength for gage lengths between 3.5 and 10.0 inches.

Figure 3 contains load-displacement curves from representative tests with gage lengths from 0.5 to 5.5 in. Diverging strain values from the front and back gages as seen for the 3.5 and 5.5 in. specimens indicate buckling. This buckling failure mode can also be seen in photographs taken during testing as shown in Figure 4. The 3.5 in specimen can be seen to have buckled out of plane in the photograph taken 0.001 before failure. After failure, the specimen contains many delaminated ply groups and therefore appears to have failed in a brooming failure mode [15]. The curves in Figure 3 indicate that at gage lengths below 3.5 in. buckling no longer controls failure so a different model should be used.

The strength model used for the small gage length region assumed the strength of the specimen was governed by flaws that were randomly spread throughout the material. The severity of the flaws was assumed to obey a Weibull distribution [16]. Since the flaws were randomly distributed, a larger specimen should on average contain a more severe flaw than a smaller specimen and therefore have a lower strength. The model that describes this size effect [17] is given by

$$\sigma = \sigma_{0.5}\left(\frac{0.5}{L}\right)^{1/m} \tag{4}$$

where σ is the strength at a gage length L, $\sigma_{0.5}$ is a reference strength taken as the strength at a gage length of 0.5 inches, and m characterizes the spread of the Weibull distribution of flaws. This size effect model is also shown in Figure 2 and shows good correlation to the measured strength data for specimens with gage lengths less than 3.5 inches. The reference strength value and the Weibull spread were determined to be 99.6 ksi and 10.4, respectively, by a least squares regression analysis. The measured compression strengths for this material are of the same magnitude as reported by others for similar materials [5,18].

The increase in strength with decreasing gage length as seen in the small gage length region in Figure 2 was not seen in data presented by others [18] and may be evident here because of a more uniform stress field in the gage section. A stress concentration like that caused by bonded tabs would disguise this effect because the amount of material in the elevated stress region would remain the same as the gage length changed. When efforts have been made to reduce the stress concentration at the end of the gage section, nonuniform strength has been observed [19,20]. Figure 5 shows a photograph of the edge of a 0.5 inch gage length specimen failing. The dark spot that appeared on the edge of the specimen 4 seconds before failure was the initial failure caused by a flaw. The spot is formed when fibers in a 0° ply at the edge of the specimen, buckle outward from the edge so that they no longer reflect the incident light. After final failure, the specimen appeared very similar to the 3.5 in gage length specimen (Figure 4) which failed due to global buckling. Therefore, the appearance of a failed compression specimen does not always indicate the controlling failure mechanism. The size effect model represents the data adequately for the small gage lengths and therefore, supports the theory that the flaw distribution in the laminate governs compressive strength. This model, however, does not provide information about the form of the flaw. Therefore, no insight is gained as to how strength might be improved or how the strength will be affected by other parameters such as environment.

Wisnom [21] has proposed a model for compression strength of a 0° ply, σ^o, based on the collapse of misaligned 0° fibers. This model is represented by the equation

$$\sigma^o = \frac{G_m \gamma}{V_m(\gamma + \alpha)} \tag{5}$$

where G_m is the secant shear modulus of the matrix material, α is the initial fiber misalignment, and γ is the composite shear strain which produces additional fiber misalignment. V_m is the matrix volume fraction, which is assumed to be the complement of the fiber volume fraction or $(1-V_f)$. This is a nonlinear equation since both G_m and γ are functions of the compressive stress. The equation assumes that at some critical stress a small amount of additional loading will reduce the matrix secant modulus so that the additional stress cannot be supported, and the composite therefore collapses.

The application of the fiber collapse model requires a shear stress-strain curve for the neat resin. The shear response of the 3501-6 matrix [22] is shown in Figure 6 under both room temperature/dry and hot/wet conditions. The hot/wet results originally presented in Reference 22 were at 200°F. These results were transformed to 180°F using a Richard-Blacklock interpolation [23]. The shear response of the toughened 8551-7 resin [24] is also presented in this figure. A polynomial least squares regression line was fit to each set of data and expressions for the secant moduli, G_m, were calculated. The critical stress can be found numerically by incrementing the matrix shear strain γ_m. The corresponding G_m and composite shear strain ($\gamma = \gamma_m V_m$) were then found and substituted into Equation 5. As the matrix shear strain is increased, the stress required to produce the strain will increase to a point and then fall off due to decreasing matrix modulus and increasing fiber misalignment. The peak stress is the predicted strength of the 0° ply. The predicted 0° ply strengths, σ^o, for 3501-6 and 8551-7 composites were calculated for a variety of initial misalignments as shown in Figure 7.

The fiber collapse model can be used in combination with the size effect model by assuming that the critical flaws in the composite are regions where the fibers are not aligned well with the loading axis. At smaller gage lengths there is less material in the gage section so the chance of having as large a fiber misalignment present would be less and the average strength would be higher. The reference laminate strength, $\sigma_{0.5}$, for this 3501-6 quasi-isotropic laminate was calculated from the test data to be 99.6 ksi, as reported earlier. The stress in the 0° ply was calculated using laminate theory to be 2.46 times the average stress. The lamina properties used in this analysis are presented in Table 1. Therefore, the reference strength of 0° ply, $\sigma^{o}_{0.5}$. is 245 ksi. This reference strength corresponds to a fiber misalignment of 1.5° as indicated by the RT/DRY 3501-6 curve in Figure 7. This fiber misalignment is comparable to reported measurements of fiber misalignment between 0.7° and 2° [25]. Although the moisture content in the specimens which were tested under ambient conditions was measurable (see Table 2), it was considerably less than the saturated specimens and was considered insignificant allowing the comparison to the RT/DRY fiber collapse results. This combination of the fiber collapse and size effect models will be used to analyze the compression strengths of the different materials subjected to different environmental conditions.

COMPARISON OF STITCHED AND TOUGHENED MATRIX COMPOSITES

The compression strength is plotted in Figure 8 versus gage length for the baseline, stitched and toughened matrix materials. The thickness of these laminate are somewhat different (see Table 2) which affects their compression strength. Strength is believed to provide the best parameter of comparison because it is directly related to how much structural weight will be needed to support a given load since the densities of the materials are basically the same. The differences in thickness among the different materials , which also affects E and V_f, is a characteristic of the different material forms.

In Figure 8, the measured strength of the different materials is plotted along with the results from the models. The models discussed in the last section appear to do a good job of modeling all three material types. The parameters used in these models are presented in Table 3. In the buckling region, the compression strength does not seem to be affected much by either stitching or by matrix toughness since all three curves fall close together. The stitched composite does appear slightly stronger in this region, but this difference is due to the stitched laminate being slightly thicker because of the stitching. The buckling strength is especially sensitive to the thickness because of its influence on the bending moment of inertia.

In the small gage length region, the stitched laminate's strength is consistently about 20% below that of the baseline. This is assumed to be largely due to the stitches causing perturbations in the 0° plies. An increased fiber misalignment from 1.5° to 2.5° due to the stitching could have caused the observed drop in strength as indicated by the 3501-6 RT/DRY curve in Figure 7. Figure 9 shows fibers in a lamina curving around a stitch and shows that a 2.5° fiber misalignment is actually a conservative value. The failure of a stitched specimen with a 0.5 in gage length is shown in Figure 10. The photographs shows damage in the laminate before failure which is extending perpendicularly across the specimen. This damage is following the line of a stitch which lies just below the surface. This supports the assumption that stitching causes local misalignments of the 0° fibers and hence lowers the strength of the composite. After failure, the specimen appears to have failed in a 45° shear band. This post failure appearance is also typical of the longer stitched specimens that buckled, again showing that post failure appearance is not a good indication of the cause of failure.

The toughened matrix appears to cause a small increase in strength as shown in Figure 8. This is somewhat surprising since the lower stiffness of the 8551-7 matrix shown in Figure 6 causes the fiber collapse model to predict a lower strength for this material. The difference may be due to a difference in fiber misalignment angles. The baseline material is a resin transfer molded uniweave. The small transverse weave of the uniweave is intended to curve around the tows in the primary direction, but a small amount of crimp may still take place. Also, during the RTM process, when resin is pumped through the dry fiber material, fibers may tend to move somewhat therefore affecting the fiber alignment. The fibers in the toughened matrix material may therefore be straighter than that of the unstitched uniweave. A change in fiber misalignment angle from 1.5° to 1.0° would account for this difference in strength as indicated by the horizontal distance between the 3501-6 and 8551-7 RT/DRY curves of Figure 7. The tape material may also be more uniform as indicated by the low slope of the size effect model curve in Figure 8. This might indicate better control of the processing of the tape material.

The failure of the tape material appears very similar to that of the baseline material. Occasionally near failure, a progression of delaminations were seen in the toughed and baseline materials, as shown in Figure 11. The photographs of the progressive failure gives insight into how the brooming failure develops. However, brooming is not believed to be the true cause of failure. The models worked equally well for the baseline, toughened, and stitched composite materials even though the progressive delamination failure was never seen in the stitched material. Also, for the shortest gage lengths, failure in the toughened and base line laminates would occasionally develop as a shear band similar to that seen for the stitched composites. The change in strength in this region of the baseline and toughened matrix composites was similar to that of the stitched material where no transition in failure appearance was seen. The progressive delaminations were therefore believed to be caused by misaligned fibers which collapsed and then caused the delaminations. Therefore, stitching or tougher matrix systems are not expected to affect compression strength due to their increased delamination toughness but may affect it due to their influence on fiber alignment and fiber support.

The strength results from the $(0/45/0/\text{-}45/90/\text{-}45/0/45/0)_S$ laminates are shown in Figure 12. The trends are similar to those for the quasi-isotropic laminate. In the buckling region, the stitched panel appears slightly stronger than the baseline or toughened panels due to the increased thickness of the panel. In the nonbuckling region, a 20% decrease in strength is seen and again is assumed due to increased fiber misalignment from stitching. The strength of the toughened matrix material is again in the range of the untoughened baseline material. The appearance of the failure was also similar to that seen for the quasi-isotropic laminates of the different materials. A larger change in strength with gage length is seen for the toughened tape material than the baseline uniweave material. This is the opposite trend from that seen for the quasi-isotropic specimens and would indicate that the tape material had a larger distribution of flaws than the uniweave.

The buckling strength of the $(0/45/0/\text{-}45/90/\text{-}45/0/45/0)_S$ laminate is significantly below that of the quasi-isotropic laminate at the same gage length. This is due to the sensitivity of buckling strength to specimen thickness. The excellent fit of the model to the data in both cases indicates that the strength in this region is truly governed by the global buckling response. The rotational spring stiffness β was changed for the modeling of the thinner laminates to 4000 in-lb/rad, because the thinner laminates did not provide as much bending constraint at the grip as the thicker laminate. The shear modulus for the $(0/45/0/-45/90/-45/0/45/0)_s$ laminates was calculated using the laminate analysis to be 0.75 Msi.

In the non-buckling region, one might expect the critical stress in the 0° plies, $\sigma^{o}_{0.5}$, for the same material to be the same for the different laminate types. Figure 13 plots $\sigma^{o}_{0.5}$ for the different materials and the different laminates. The figure shows that the strengths of the 0° plies in the $(0/45/0/-45/90/-45/0/45/0)_s$ laminates are consistently 15% below that from the quasi-isotropic laminate. Although surprising, this could be due to the $(0/45/0/-45/90/-45/0/45/0)_s$ laminate having a 0° ply on the outside of the laminate which may be more critical than an embedded 0° ply.

EFFECT OF HOT/WET CONDITIONS

Each material and both types of laminates were tested under hot/wet conditions as described earlier in this paper. The moisture content in each material and for each laminate is recorded in Table 2. The stitched material absorbed significantly more moisture than either the unstitched or the toughened matrix material. This was probably due to the additional resin content in this material and due to the glass stitch material allowing more moisture absorption. Another reason the stitched material's moisture content may have been higher was that even after the 45-day soak, the specimens were not completely saturated. The stitched material was more nearly saturated because it absorbed moisture much quicker, possibly due to the resin rich stitches wicking moisture to the interior of the laminate. The

8551-7 tape material absorbed less moisture than the 3501-6 uniweave. The thinner $(0/45/0/-45/90/-45/0/45/0)_S$ laminates had larger % moisture contents than the thicker quasi-isotropic laminate after the 45 day soak. This also may be due to differences in saturation level with the thinner laminate being more nearly saturated. The material for the hot/wet tests was assumed completely saturated and compared using saturated elevated temperature matrix properties.

The compression strengths of the quasi-isotropic laminates and of the $(0/45/0/-45/90/-45/0/45/0)_S$ laminates are presented in Figures 14 and 15, respectively. The trends in both cases look similar to those seen under ambient conditions, and the model strength curves fit the data well. The parameters used in generating these curves are presented in Table 3. The buckling strength curves were practically unaffected by the change in test environment. The buckling strength is primarily a function of the laminate stiffness which, as shown by the measured modulus data in Table 2, is essentially unchanged. The laminate stiffness is mainly controlled by the stiffness of the fibers which should not be affected by the hot/wet conditions. The stitched laminate again appears a little stronger in the buckling region because it is slightly thicker. In the nonbuckling region, the stitched laminate compressive strength was again almost 20% lower than the baseline unstitched uniweave. The reduction was slightly less than 20% for the quasi-isotropic laminate and slightly more for the $(0/45/0/-45/90/-45/0/45/0)_S$ laminate. The toughened matrix material is 13% and 19% higher than the baseline material under the hot/wet conditions for the quasi-isotropic and $(0/45/0/-45/90/-45/0/45/0)_S$ laminates, respectively. This is different from the ambient conditions where they were about the same. The similarity in strength for these materials at ambient conditions is postulated to be due to compensating factors: straighter fibers and a more compliant matrix in the tape material. It is not surprising that under hot/wet conditions the strengths would no longer be the same since the hot/wet environment would have a different effect on the two matrix materials.

To better evaluate the effect of the hot/wet conditions, the $\sigma^{o}_{0.5}$ for each material and each laminate were compared for the ambient and hot/wet conditions. These results are shown in Figure 16. Both the baseline and the stitched materials had about a 30% drop in strength due to the hot/wet conditions for both laminates. The drop in strength for the toughened matrix material was only about 20%.

Figure 6 also shows the shear response of the 3501-6 and 8551-7 matrix material under hot/wet conditions. The hot/wet matrix properties of the two materials were used in the fiber collapse model to predict the strengths of the 0° ply. These predictions are shown in Figure 7. Assuming fiber misalignment angles in the 1-3 degree range, these predictions suggest that a 50% drop in strength from the room temperature tests should be expected for the baseline and stitched materials, and a 35% drop should be expected for the toughened matrix material. This predicted reduction is significantly larger than the measured reduction, but the prediction that the effect would not be as large for the toughened matrix composite was correct. The predicted reduction may be greater than the measured reduction because the ambient specimens were assumed to be completely dry and the hot/wet specimens were assumed to be completely saturated. Neither condition was strictly true, so the changes in matrix properties due to moisture were over estimated. The moisture effect however should be smaller than the effect of temperature [22, 24].

The strength under hot/wet conditions of the 0° ply in the quasi-isotropic laminate again was consistently higher than in the (0/45/0/-45/90/-45/0/45/0)$_S$ laminate. Although not noted on Figure 16, $\sigma^{o}_{0.5}$ for the two baseline material laminates differed by 13% under hot/wet conditions. This is consistent with the 14% difference found under ambient conditions, as was shown in Figure 13, and again may be due to the (0/45/0/-45/90/-45/0/45/0)$_S$ laminate having 0 external plys. The difference in $\sigma^{o}_{0.5}$ between the two laminates was 20% for the stitched material and only 8% for the toughened matrix material under hot/ wet conditions as compared to differences at ambient conditions of 15% and 13%, respectively. The discrepancy between the ambient and hot/wet values for the stitched and toughened materials may simply be due to experimental scatter.

CONCLUDING REMARKS

The effect of the trade-off between stitching and toughened matrix systems on the compression property of composite laminates was determined at both ambient and hot/wet conditions and for a large range of unsupported gage lengths. The compressive strength of a stitched uniweave composite with a brittle epoxy (3501-6) and of an unstitched tape composite containing a toughened epoxy (8551-7) were compared to a baseline material made of unstitched uniweave with the brittle epoxy matrix. This comparison was made for two laminates: a 48-ply quasi-isotropic laminate and a thinner 18-ply (0/45/0/-45/90/-45/0/45/0)$_S$ laminate which contained a larger portion of 0° plies.

If a compression specimen was long enough to buckle, the important material parameters were the laminate stiffness and thickness as indicated by the buckling model. The stitched material which had a slightly reduced modulus from the baseline material actually carried more load because of the laminate's increased thickness. No effect of the hot/wet environment was observed when buckling governed failure.

When the test specimens were short (<3.5 inches), the specimens failed before buckling occurred. The strength of the composite was not constant in this region but increased as the gage length decreased. This increasing strength was believed to be due to a random distribution of flaws within the material which causes larger specimens to have a lower strength on average. The critical flaw was assumed to be misaligned fibers. A model that predicts strength based on the fiber misalignment angle and the matrix nonlinear shear stress-strain curve was used to predict strengths. The predicted results agreed well with measured values.

An observed 20% reduction in the strength of the stitched material from that of the baseline materials was attributed to a small increase in fiber misalignment caused by the stitching. The strength of the toughened tape material was approximately the same as the baseline material but the similarity in strength is believed to be due to compensating effects of straighter fibers and a lower modulus matrix. The resistance to delamination gained by stitching or by increased matrix toughness is not believed to influence compression strength. Delaminations that were observed during the failure of the baseline and toughened tape materials were believed to develop after failure was initiated by the collapse of misaligned fibers. The effect of stitching and of the toughened matrix was approximately the same for both quasi-isotropic and $(0/45/0/-45/90/-45/0/45/0)_S$ laminates but the strength of the critical 0° plies was calculated to be 15% higher for the quasi-isotropic laminate, on average.

The hot/wet environment caused a reduction in strength for all materials, but the effect was somewhat larger for the baseline and stitched materials which had the more brittle matrix. The decrease in strength was around 30% for these materials and only 20% for the toughened matrix material. The smaller effect on the toughened matrix composite was predicted by the model. The effect of moisture was the same for both laminates.

Although this paper shows that the compression strength is adversely affected by stitching (if buckling does not cause failure), it is only one of many properties which must be evaluated when choosing a material system. The results of this study also indicate that care must be taken when comparing compression data because strength values can change with gage size. The results also showed that the appearance of a failed specimen is not a good indication of the cause of compression failure. Finally, the 30% decrease in strength due to stitching showed just how sensitive the compression strength is to fiber misalignment.

REFERENCES

1. *Toughened Composites: SYMPOSIUM ON TOUGHENED COMPOSITES, ASTM STP 937*, Johnston, N.J., Ed., American Society for Testing and Materials, Philadelphia, 1985.

2. Dow, M.B.; Smith, D.L.; and Lubowinski, S.J.: "An Evaluation of Stitching Concepts for Damage-Tolerant Composites," *Fiber-Tex 1988 Conference Proceedings,* NASA CP-3038, 1989, pp. 53-73.

3. Jang, B.Z.; Shih, W.K.; and Chung, W.C.: "Mechanical Properties of Multidirectional Fiber Composites," *Journal of Reinforced Plastics and Composites*, Vol. 8, November 1989, pp. 538-464.

4. Lubowinski, S.J.; Guynn, E.G.; Elber, W.; and Whitcomb, J.D., "Loading Rate Sensitivity of Open-Hole Composite Specimens in Compression," *Composite Materials: Testing and Design,* Garbo, S.P., Ed., American Society for Testing and Materials, Philadelphia, 1990, pp. 457-476.

5. Berg, J.S.; and Adams, D.F.: "An Evaluation of Composite Material Compression Test Methods," *Journal of Composites Technology & Research*, Vol. 11, No. 2, Summer 1989, pp. 41-46.

6. Tan, S.C., "Stress Analysis and the Evaluation of Celanese and IITRI Compression Test Specimens," *Composite Materials in Transition,* Proceeding of the American Society for Composites, E. Lansing, Michigan, June 1990, pp. 827-838.

7. Wisnom, M.R.: "Effect of Shear Stresses in Indirect Compression Tests of Unidirectional Carbon Fiber/Epoxy," *AIAA Journal*, Vol. 29, No. 10, October 1991, pp. 1692-1697.

8. Cano, R.J.; and Dow, M.B.: "Properties of Five Toughened Matrix Composite Materials," NASA TP-3254, October 1992.

9. "Strain Gage Applications with M-Bond AE-10/15 and M-Bond GA-2 Systems," Instruction Bulletin B-137-15, Micro-Measurements, Raleigh, NC, 1979.

10. Lauraitis, K.N.; and Sandorff, P.E.: "The Effect of Environment on the Compressive Strengths of Laminated Epoxy Matrix Composites," AFML-TR-79-4179, Wright-Patterson Air Force Base, Ohio, December 1979.

11. Wung, E.C.J.; and Chatterjee, S.N.: "On the Failure Mechanisms in Laminated Compression Specimens and the Measurement of Strengths," *Journal of Composite Materials*, Vol. 26, No. 13, 1992, pp. 1885-1914.

12. Timoshenko, S.: *Theory of Elastic Stability*. New York: McGraw-Hill Book Co., Inc., 1936, p. 140.

13. Newmark, N.M.: "A Simple Approximate Formula for Effective End-Fixity of Columns," *Journal of the Aeronautical Sciences.*, Vol 16, No. 2, AIAA, Easton, PA, 1949, p. 116.

14. Murri, G.B.; Salpekar,.S.A.; and O'Brien, T.K.: "Fatigue Delamination Onset Prediction in Unidirectional Tapered Laminates," *Composite Materials: Fatigue and Fracture, Vol. 3, ASTM STP 1110*, O'Brien, T.K., Ed., American Society for Testing and Materials, Philadelphia, 1991, pp. 312-339.

15. Odom, E.M.; and Adams, D.F.: "Failure Mode of Unidirectional Carbon/Epoxy Composite Compression Specimens," *Composites*, Vol. 21, No. 4, July 1990, pp. 289-296.

16. Weibull, W.A.: "A Statistical Distribution Function of Wide Applicability," *Journal of Applied Mechanics*, Vol. 18, 1951, p. 293.

17. Hitchon, J.W.; and Phillips, D.C.: "The Effect of Specimen Size on the Strength of CFRP," *Composites*, Vol. 9, 1978, pp. 119-124.

18. Adams, D.F.; and Lewis, E.Q.: "Influence of Specimen Gage Length and Loading Method on the Axial Compressive Strength of a Unidirectional Composite Material," *Experimental Mechanics*, March 1991, pp. 14-20.

19. Haeberle, J.; and Matthews, F.L.: "Studies on Compressive Failure in Unidirectional CFRP using an Improved Test Method," *Developments in the Science and Technology of Composite Materials,* J. Füller et. al., Eds. Proceedings of the 4th European Conference on Composite Materials, Elsevier Applied Science, Stuttgart, FRG, September 1990, pp. 517-521.

20. Wisnom, M.R.: "The Effect of Specimen Size on the Bending Strength of Unidirectional Carbon Fibre-Epoxy," *Composite Structures*, Vol. 18, 1991, pp. 47-63.

21. Wisnom, M.R.: "The Effect of Fibre Misalignment on the Compressive Strength of Unidirectional Carbon Fibre/Epoxy," *Composites*, Vol. 21, No. 5, September 1990, pp. 403-407.

22. Adams, D.F.: "A Micro Mechanics Analysis of the Influence of the Interface on the Performance of Polymer Matrix Composites," *Journal of Reinforced Plastics and Composites*, Vol. 6, January 1987, pp. 66-88.

23. Richard, R.M.; and Blacklock, J.R.: "Finite Element Analysis of Inelastic Structures," *AIAA Journal*, Vol. 7, No. 3, 1968, pp. 432-438.

24. Coquill, S.L.; and Adams, D.F.: "Mechanical Properties of Several Neat Polymer Matrix Materials and Unidirectional Carbon Fiber-Reinforced Composites," NASA CR-181805, April 1989.

25. Camponeschi, E. T., Jr.: "Lamina Waviness Levels in Thick Composites and Its Effect on Their Compression Strength," *Composites: Design, Manufacture, and Application,* Tsai, S.W. and Springer, G.S., Eds., Proceedings of the Eighth International Conference on Composite Materials (ICCM/8), SAMPE, Honolulu, July 1991, No. 30-E, pp. 1-13.

26. Gipple, K.: "A Comparison of the Compression Response of Thick (6.35mm) and Thin (1.60 mm) Dry and Moisture Saturated AS4/3501–6 Laminates," DTRC-SME-90/74, David Taylor Research Center, Bethesda, MD, October 1990.

Table 1. AS4/3501-6 Lamnia Properties [26]

E_{11} (Msi)	16.6
E_{22} & E_{33} (Msi)	1.5
ν_{12} & ν_{13}	0.33
ν_{23}	0.47
G_{12} & G_{13} (Msi)	0.87
G_{23} (Msi)	0.55

Table 2. Measured Laminate Properties

	Thickness		**Density**	V_f	**Modulus**		**% Moisture**	
	in.		lb/in^3	%	Msi		%	
		Std. Dev.			Ambient	Hot/wet	Ambient	Hot/wet
Baseline								
Quasi-Isotropic	0.255	0.010	0.0579	62.3	7.18	7.23	0.17	0.69
$(45/0/-45/90/-45/0/45/0)_s$	0.100	0.004	0.0581	63.6	9.71	9.71	0.43	1.41
Stitched								
Quasi-Isotropic	0.291	0.003	0.0577	54.1	6.47	6.54	0.51	1.33
$(45/0/-45/90/-45/0/45/0)_s$	0.114	0.001	0.0578	58.5	8.69	8.64	0.58	1.63
Toughned Matrix								
Quasi-Isotropic	0.268	0.004	0.0561	57.9	6.63	6.84	0.17	0.52
$(45/0/-45/90/-45/0/45/0)_s$	0.102	0.002	0.0553	60.4	9.18	9.39	0.34	0.95

Table 3. Strength Model Parameters

	Buckling Model		Weibull Model				0° Strength	
	G_{12} (MSI)	β (in-lb/rad)	$\sigma_{0.5}$ (ksi)		m		$\sigma^{\circ}_{0.5}$ (ksi)	
			Ambient	Hot/wet	Ambient	Hot/wet	Ambient	Hot/wet
Baseline								
Quasi-Isotropic	.69	16,000	99.6	68.1	10.4	21.0	245	168
$(45/0/-45/90/-45/0/45/0)_s$	.75	4,000	118.0	82.0	15.2	22.6	210	146
Stitched								
Quasi-Isotropic	.69	16,000	80.1	56.7	8.8	18.7	197	139
$(45/0/-45/90/-45/0/45/0)_s$	.75	4,000	93.8	62.3	10.2	7.1	167	111
Toughned Matrix								
Quasi-Isotropic	.69	16,000	101.1	77.2	14.5	36.1	249	190
$(45/0/-45/90/-45/0/45/0)_s$	.75	4,000	121.4	97.7	6.5	15.3	216	174

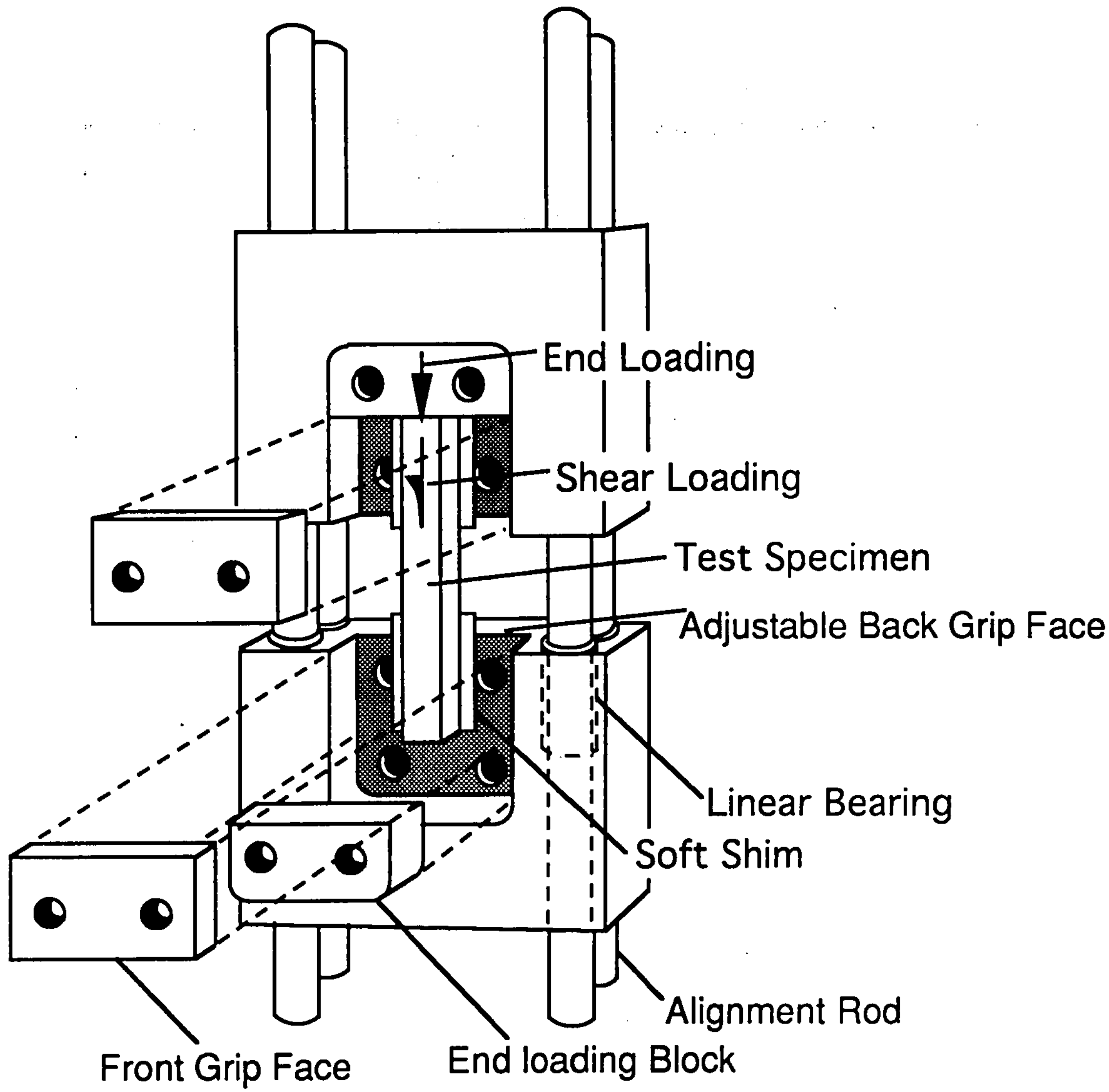

Figure 1. Linear bearing compression test fixture.

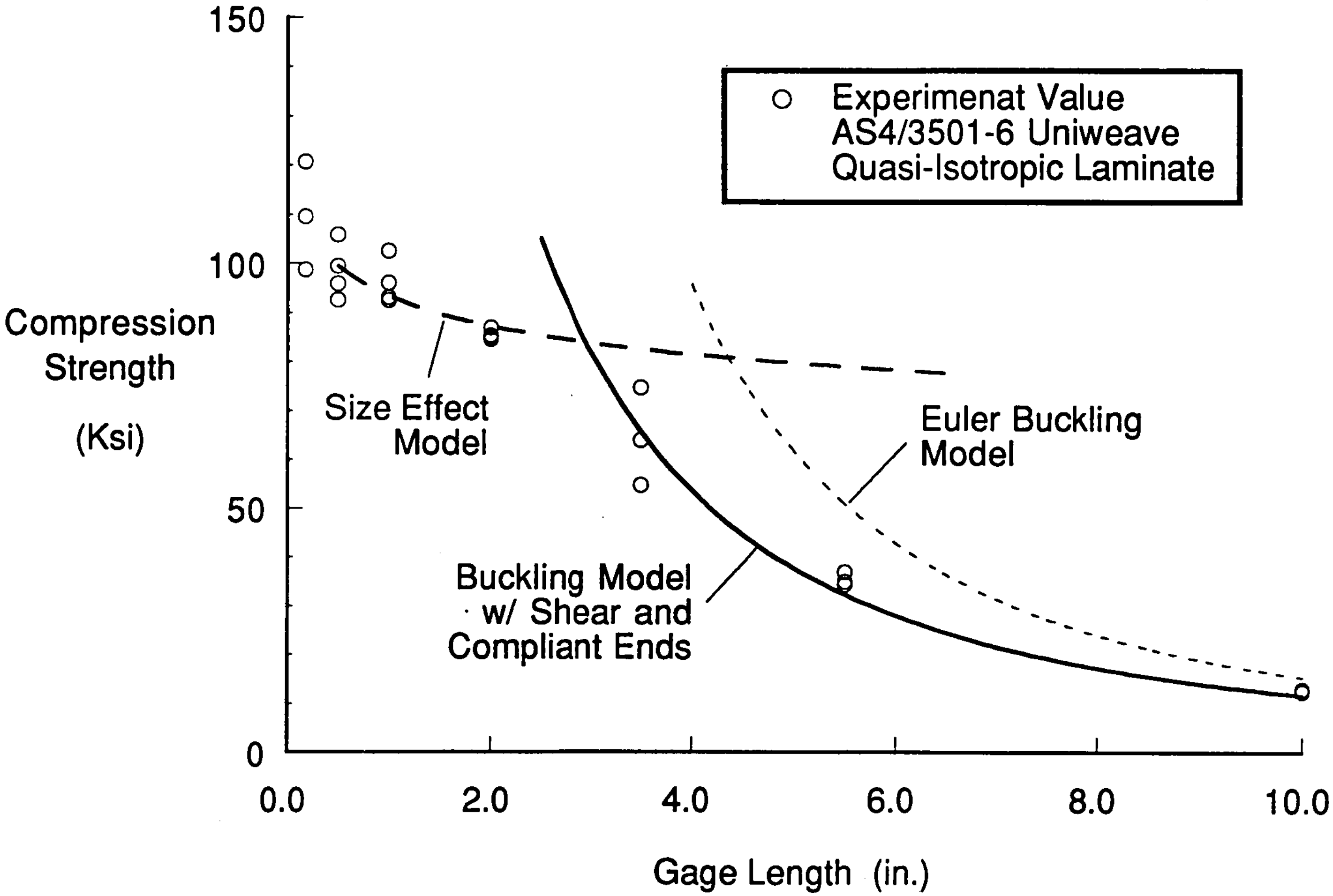

Figure 2. Compression strength models for quasi-isotropic baseline laminate.

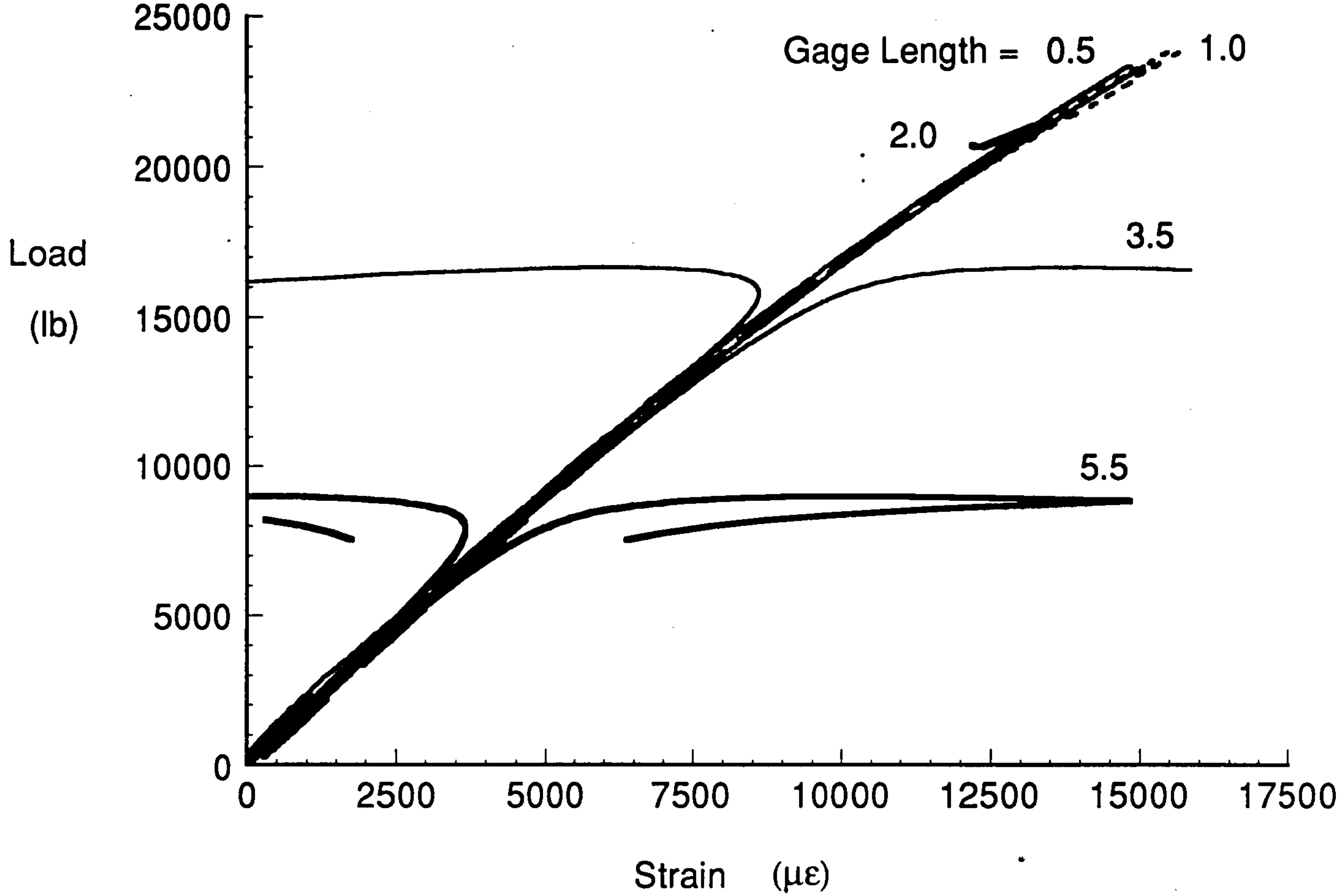

Figure 3. Loading response of baseline laminates at different gage lengths.

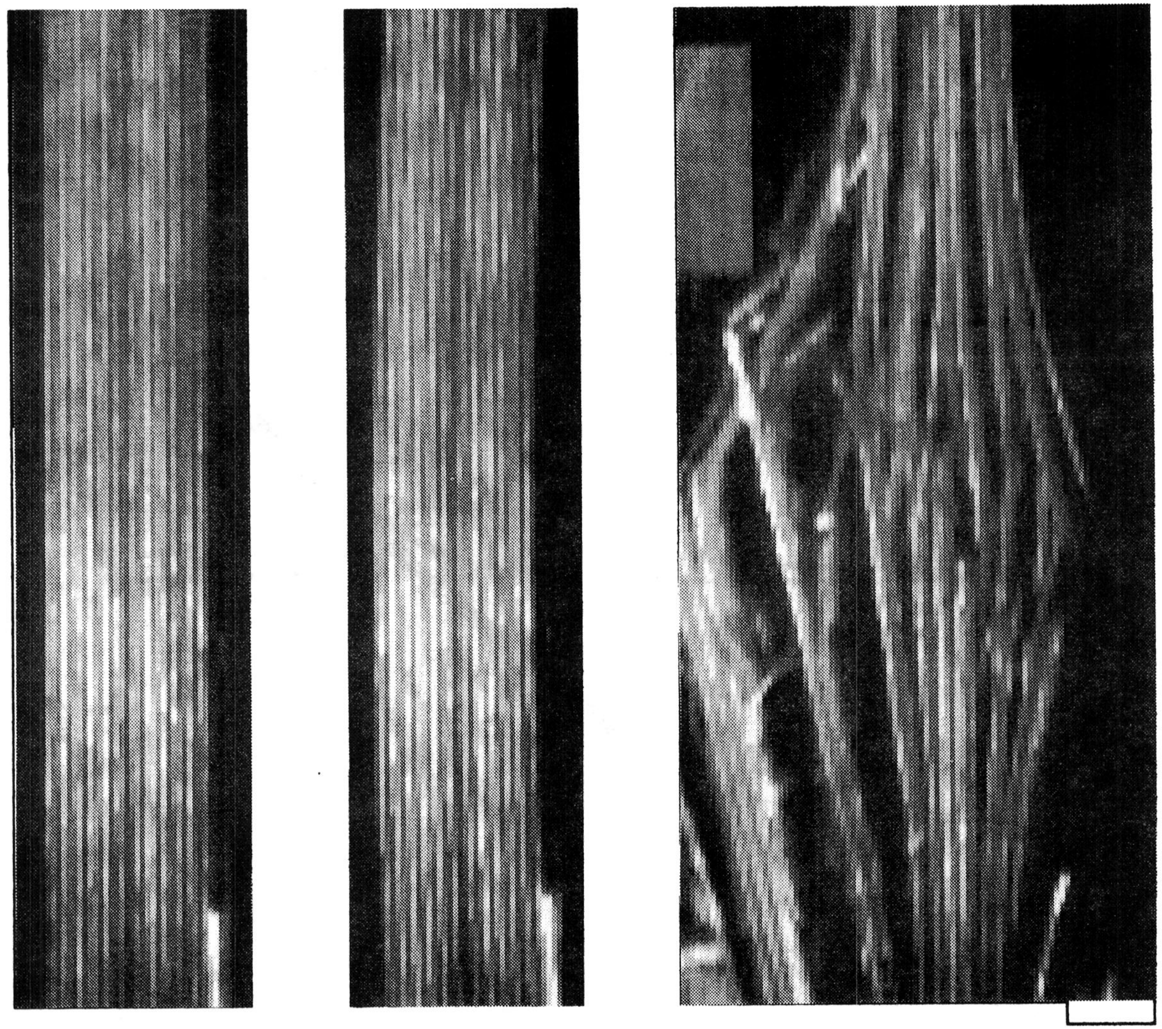

Initial | 0.001 sec Prior to Failure | Failure | 0.1 in.

Figure. 4 Buckling failure of quasi-isotropic baseline laminate with a 3.5 in. gage length.

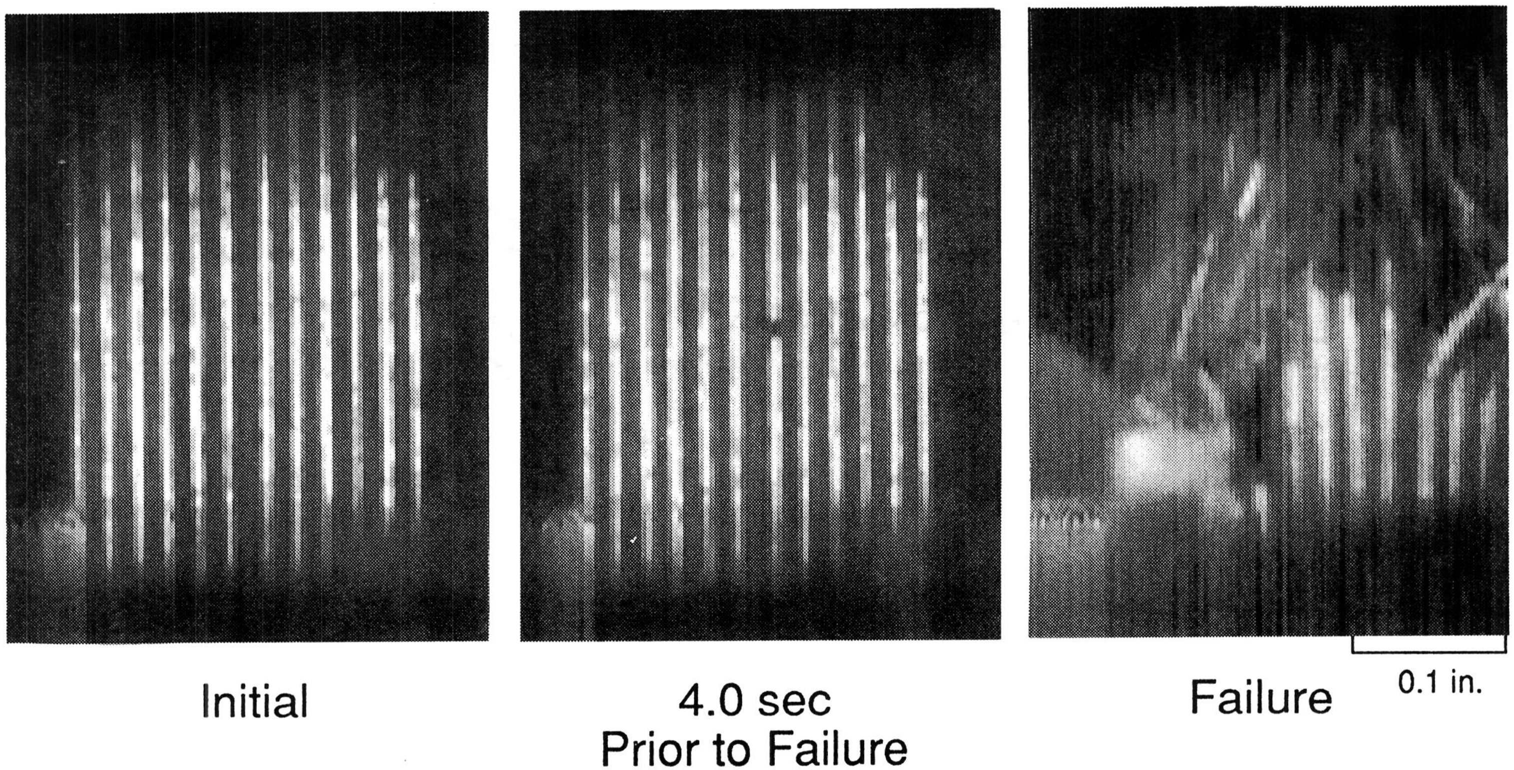

Figure. 5 Local failure in quasi-isotropic baseline laminate with a 0.5 in. gage length.

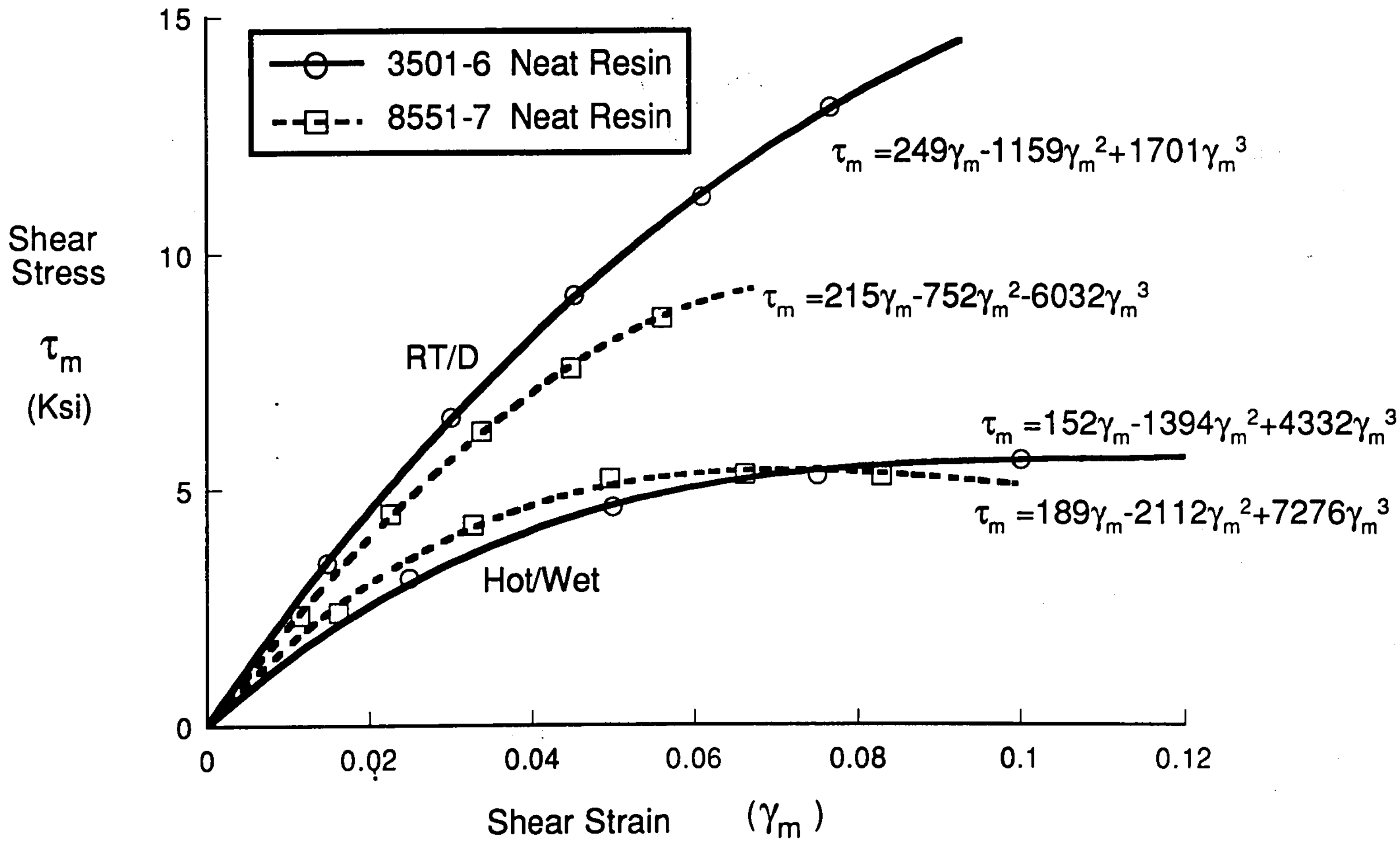

Figure 6. Shear response of 3501-6 [22] and 8551-7 [24] neat resins.

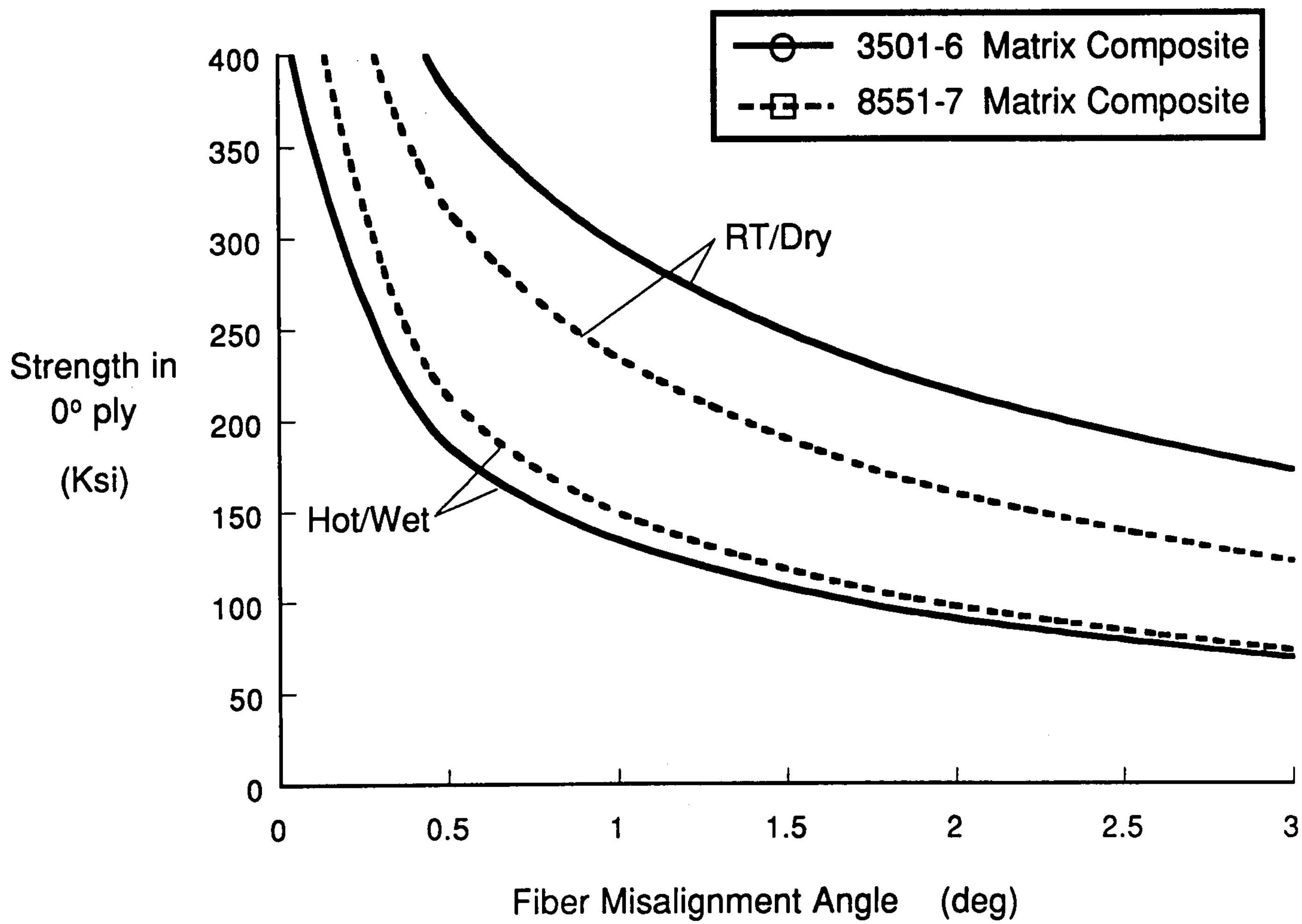

Figure 7. Strength predictions of fiber collapse model.

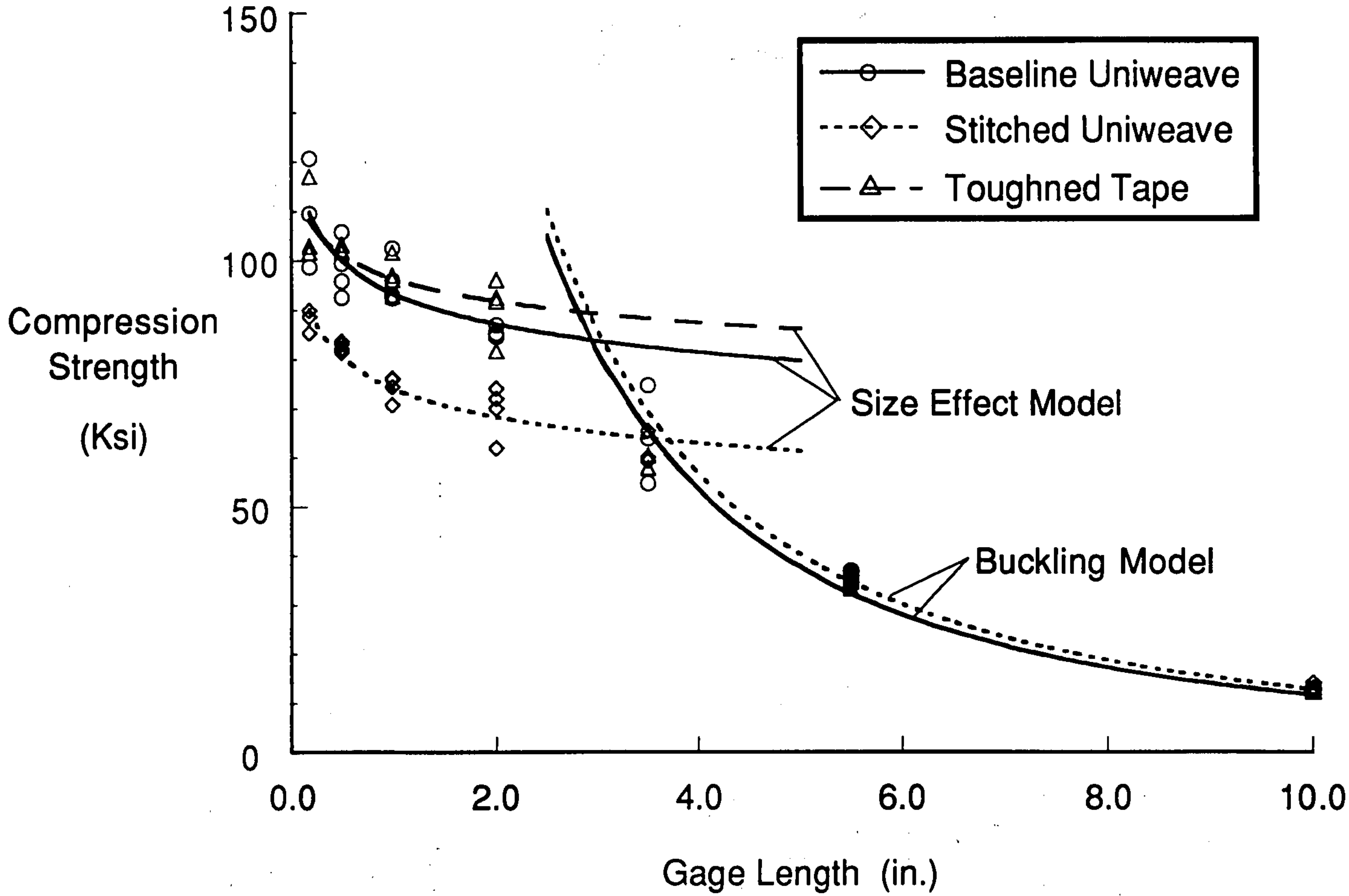

Figure 8. Compression strength of quasi-isotropic laminates under ambient conditions.

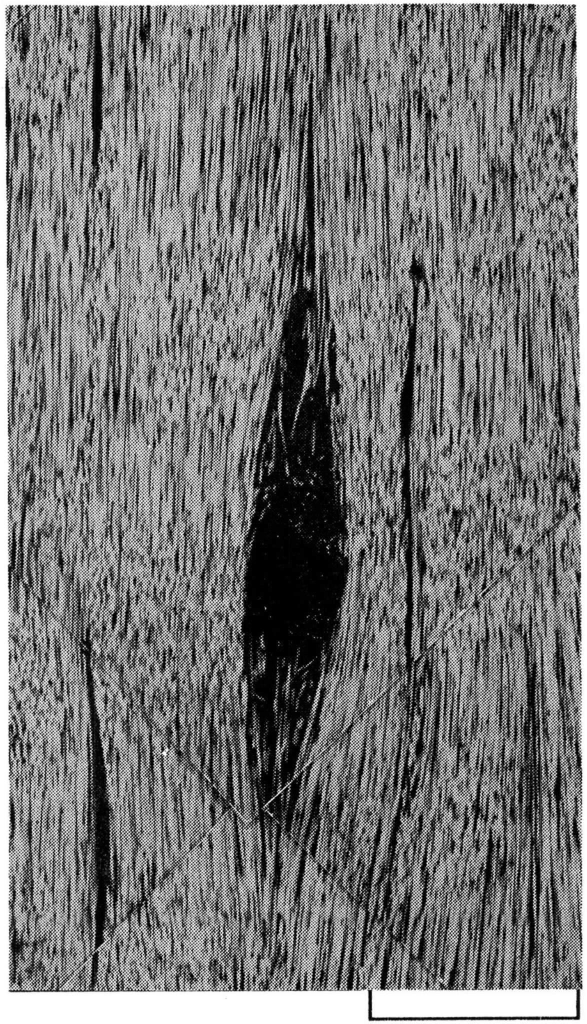

Figure 9. Fiber orientation around a stitch.

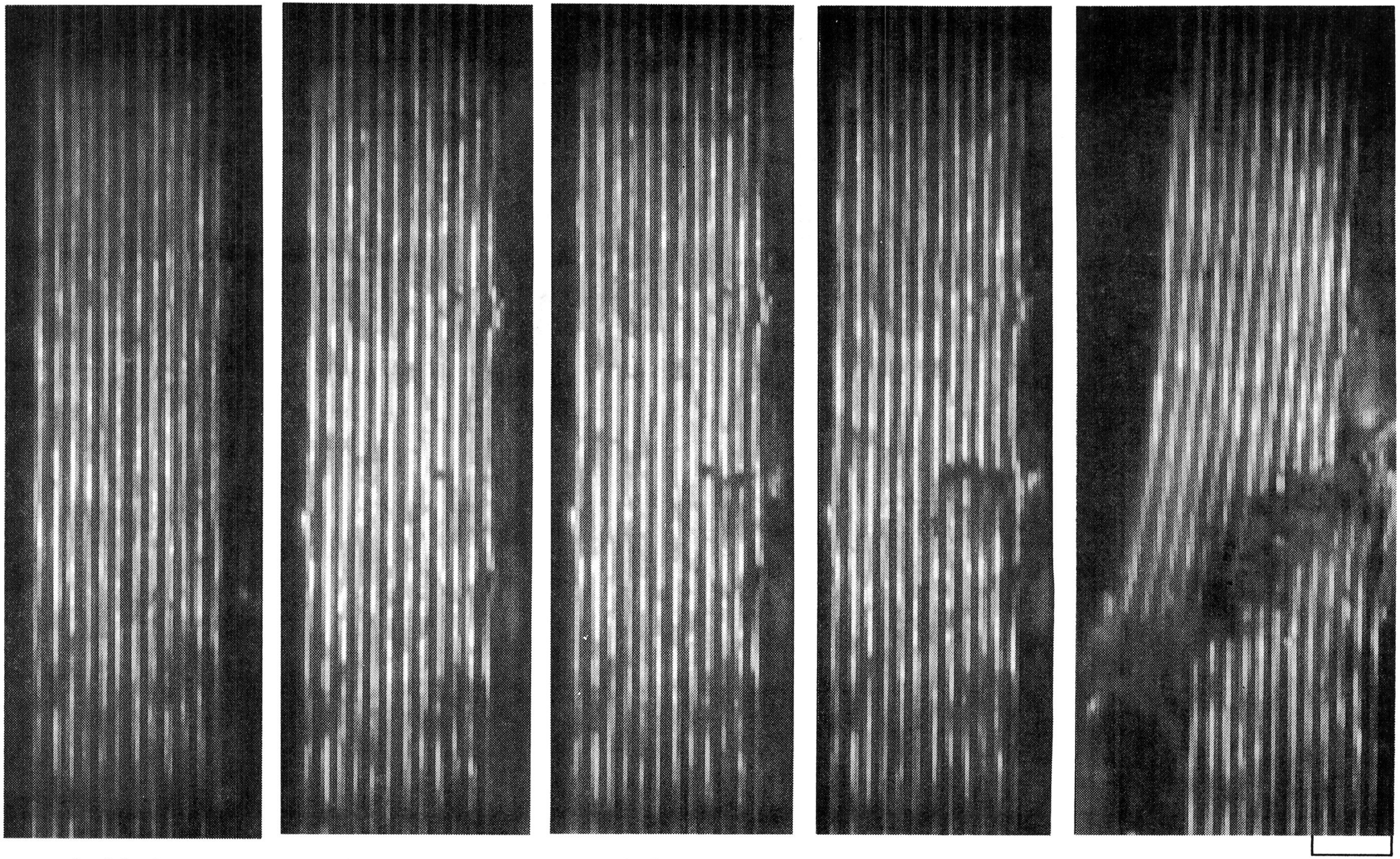

Figure. 10 Failure of quasi-isotropic stitched laminate with a 2 in. gage length

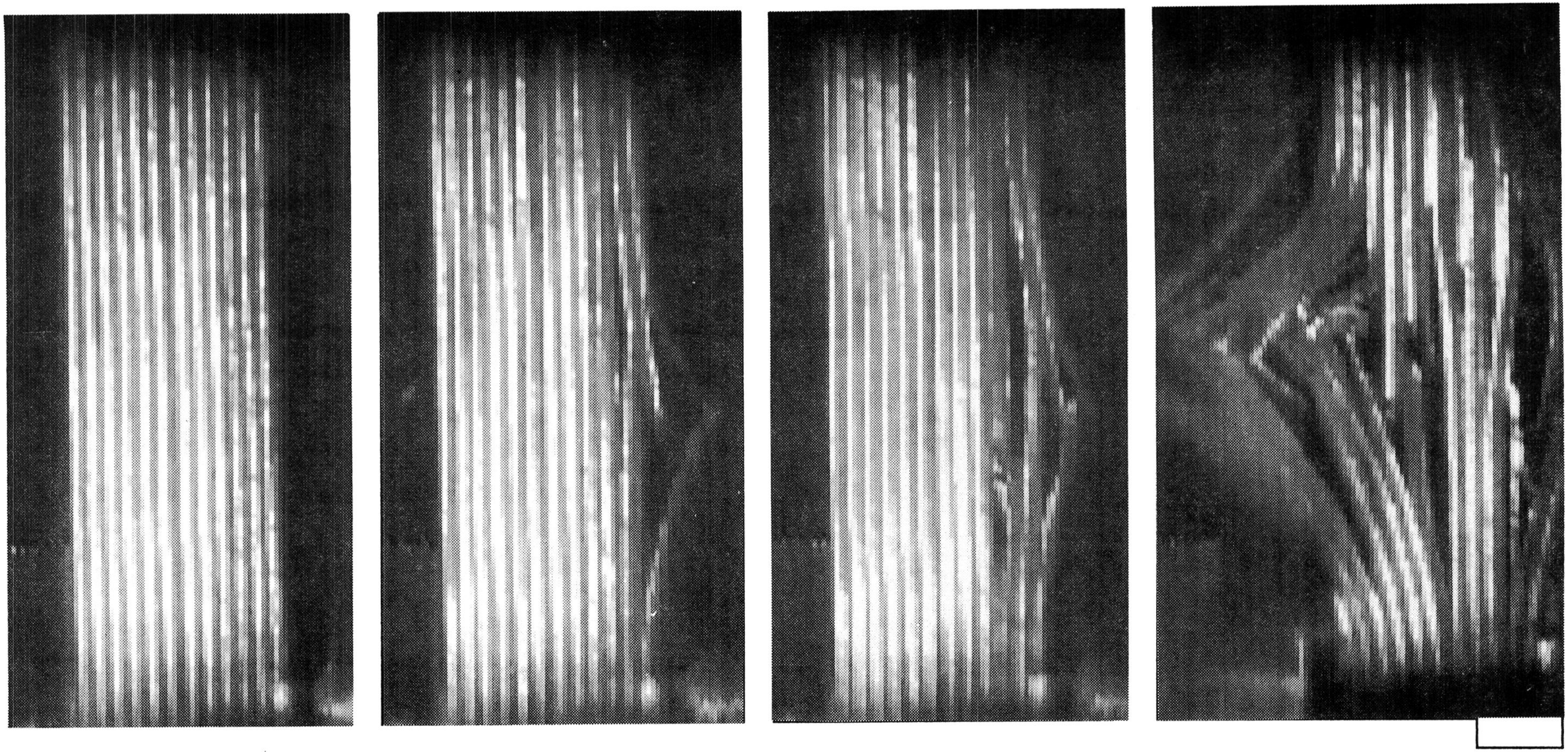

Initial | 1.6 sec Prior to Failure | 0.1 sec Prior to Failure | Failure

Figure. 11 Progressive delamination failure of toughened tape laminate with a 1 in. gage length

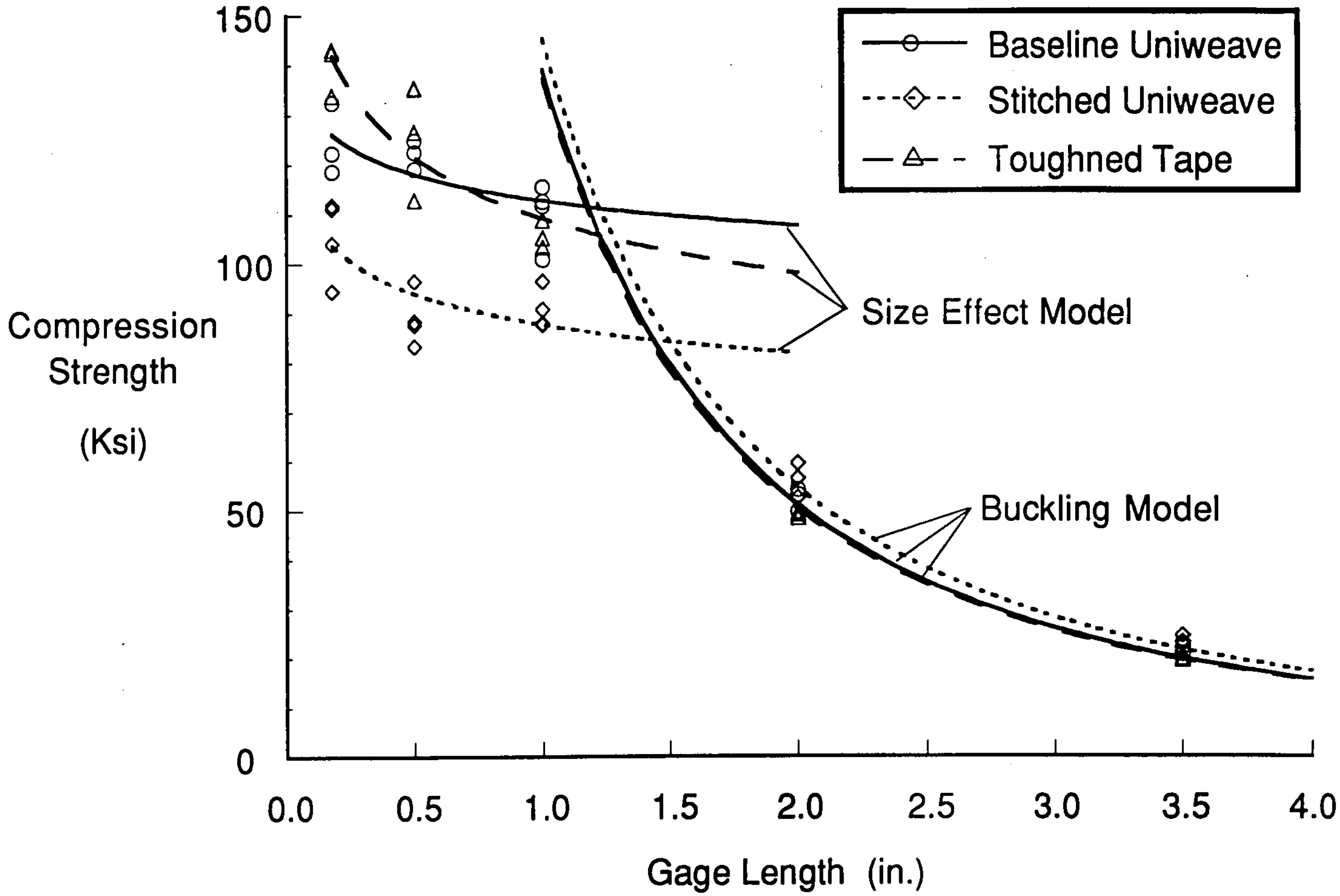

Figure 12. Compression strength of $(0/45/0/-45/90/-45/0/45/0)_s$ laminates under ambient conditions.

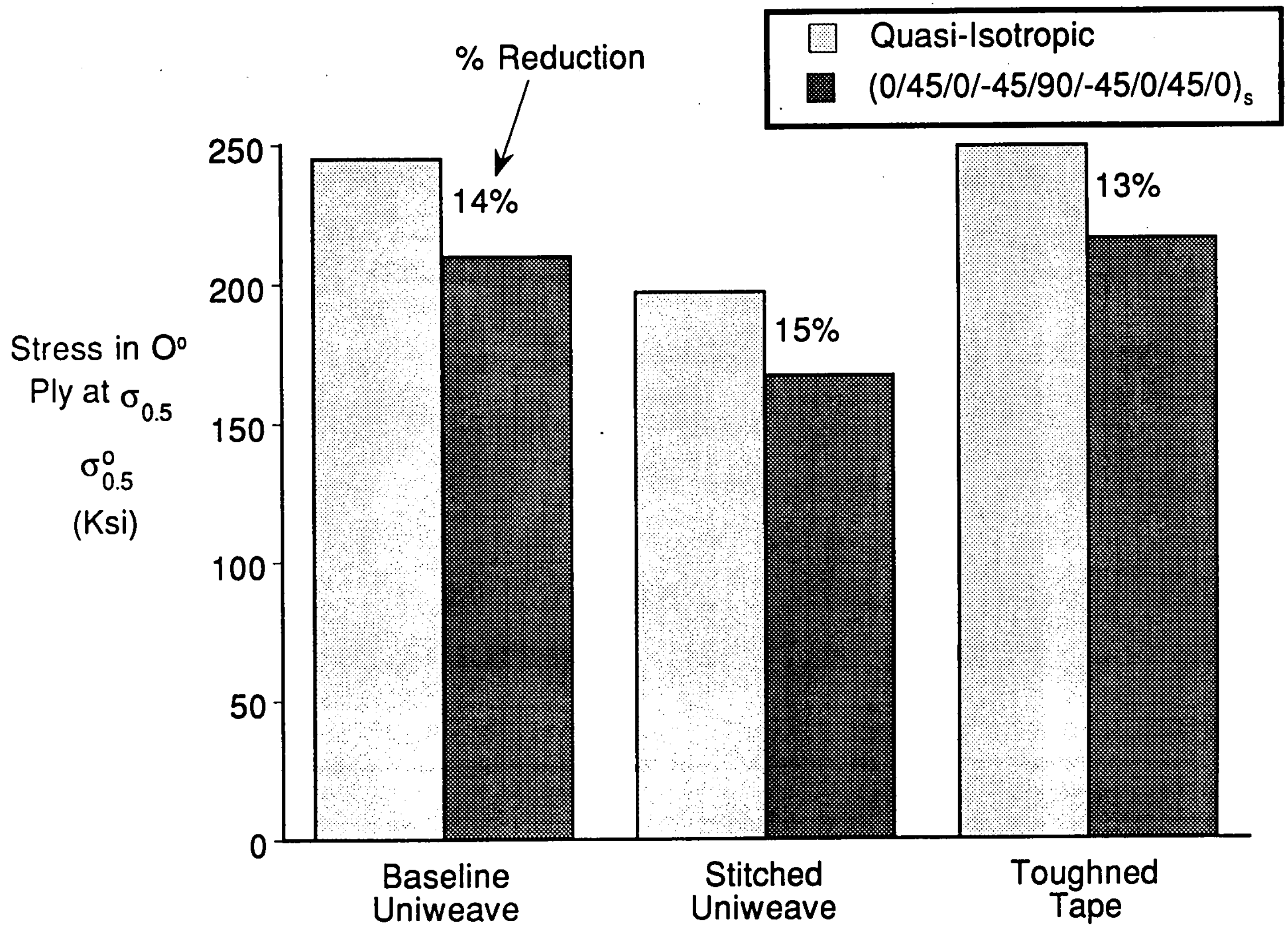

Figure 13. Comparison of the compression strength of different laminates.

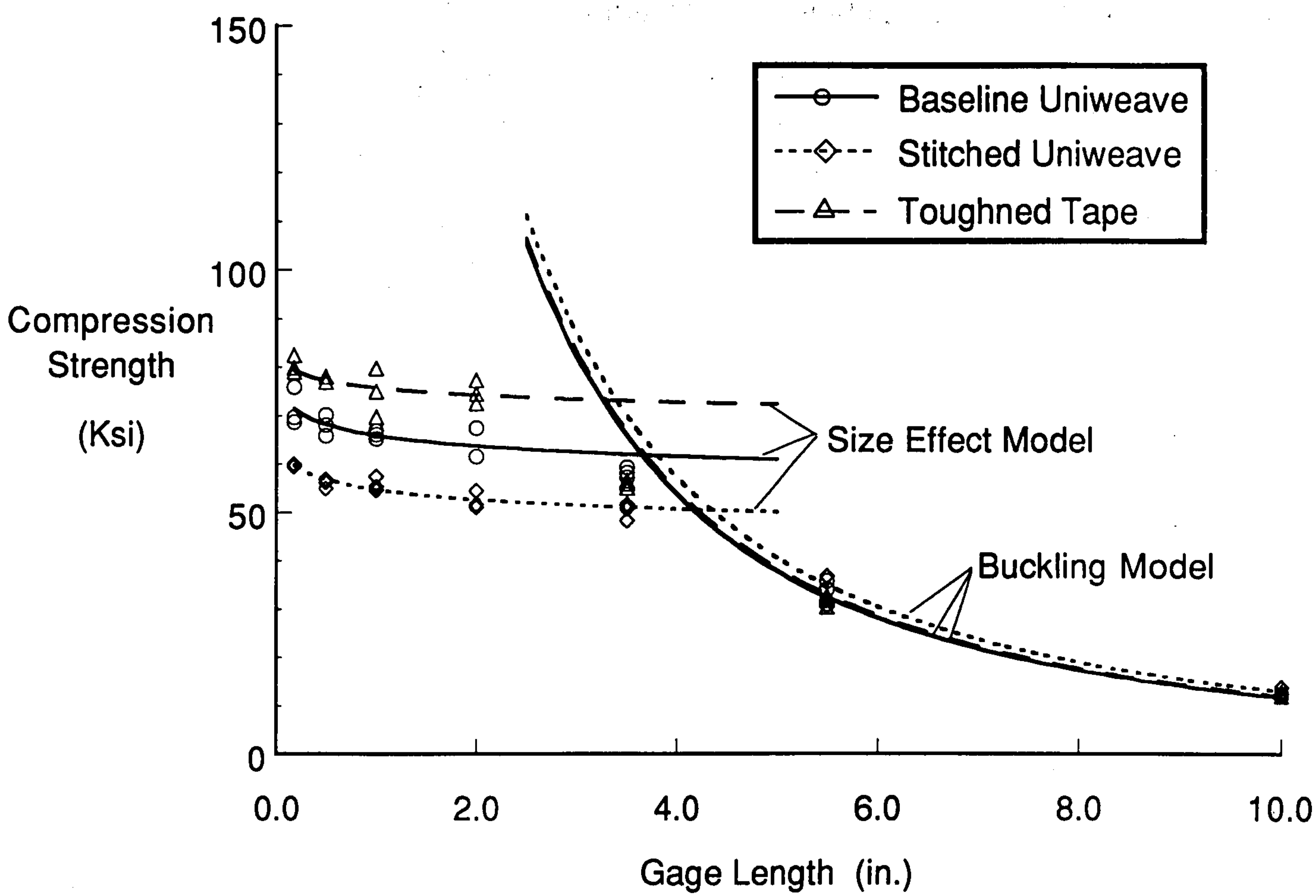

Figure 14. Compression strength of quasi-isotropic laminates under hot/wet conditions.

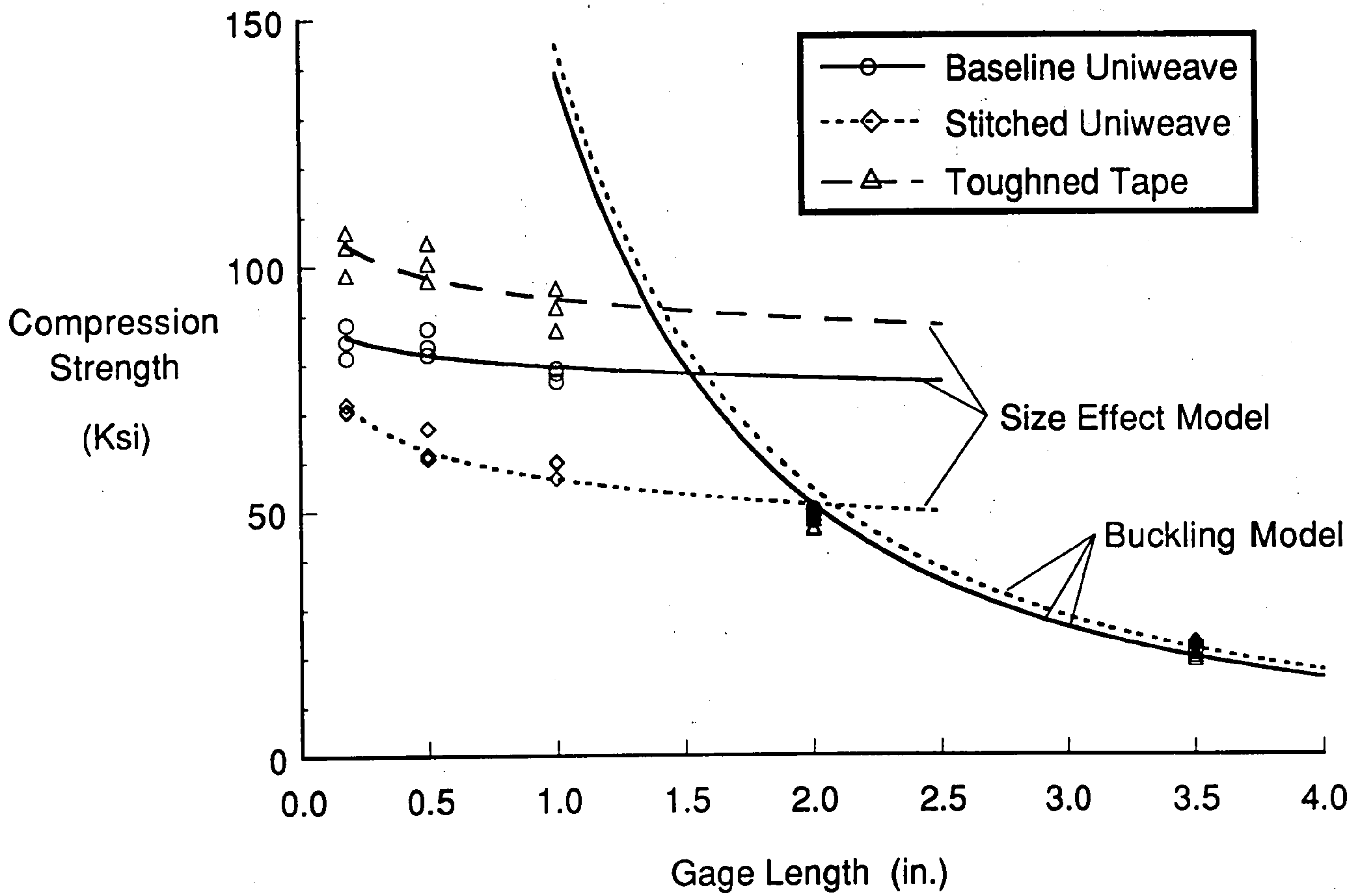

Figure 15. Compression strength of $(0/45/0/-45/90/-45/0/45/0)_s$ laminates under hot/wet conditions.

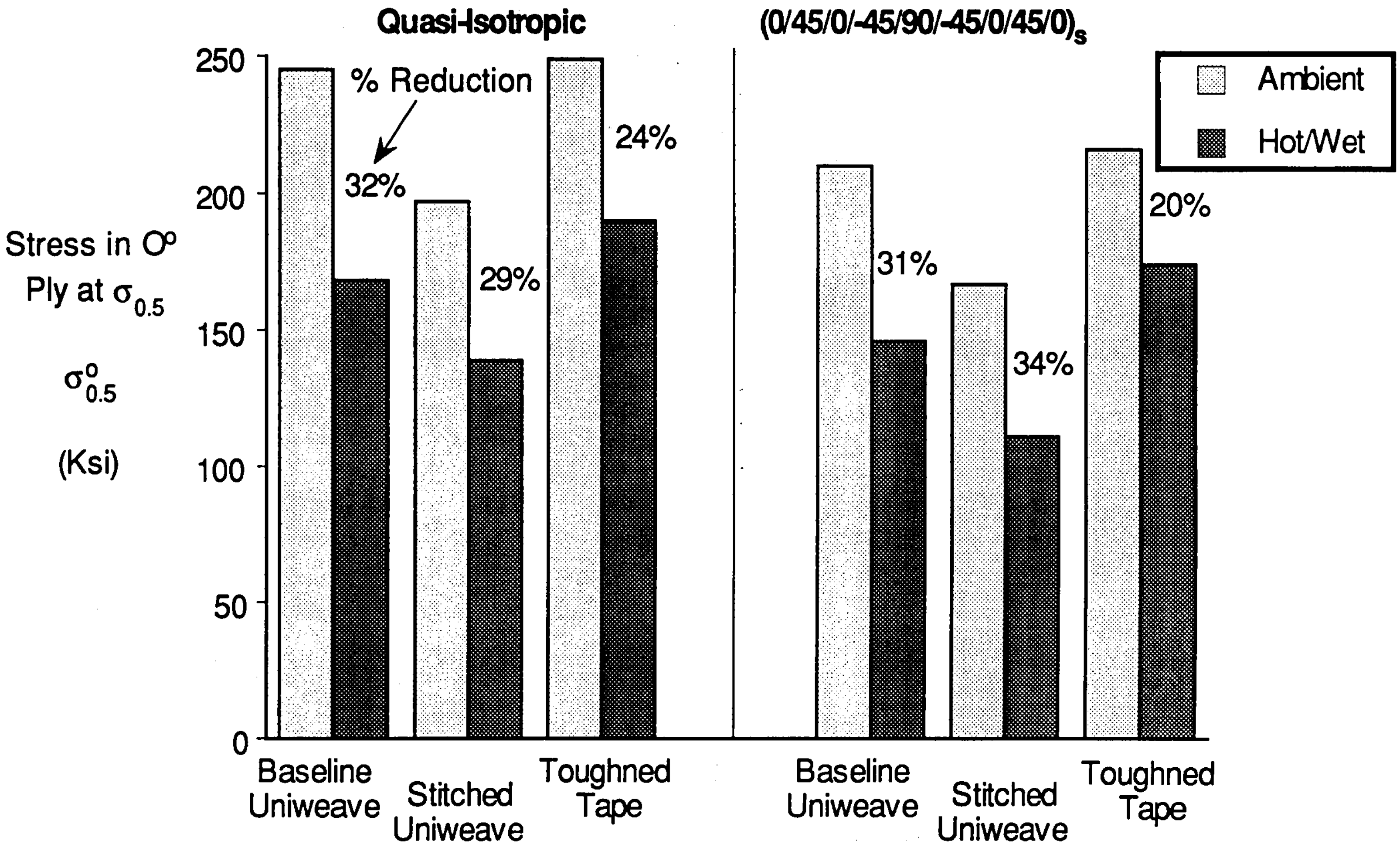

Figure 16. Effect of hot/wet conditions on compression strength.

REPORT DOCUMENTATION PAGE

Form Approved
OMB No. 0704-0188

1. AGENCY USE ONLY *(Leave blank)*	2. REPORT DATE	3. REPORT TYPE AND DATES COVERED
	April 1994	Technical Memorandum

4. TITLE AND SUBTITLE
Comparison of the Compressive Strengths for Stitched and Toughened Composite Systems

5. FUNDING NUMBERS
WU 505-63-50-04

6. AUTHOR(S)
James R. Reeder

7. PERFORMING ORGANIZATION NAME(S) AND ADDRESS(ES)
NASA Langley Research Center
Hampton, VA 23681-0001

8. PERFORMING ORGANIZATION REPORT NUMBER

9. SPONSORING/MONITORING AGENCY NAME(S) AND ADDRESS(ES)
National Aeronautics and Space Administration
Washington, DC 20546-0001

10. SPONSORING/MONITORING AGENCY REPORT NUMBER
NASA TM 109108

11. SUPPLEMENTARY NOTES

12a. DISTRIBUTION/AVAILABILITY STATEMENT
Unclassified - Unlimited

Subject Category 24

12b. DISTRIBUTION CODE

13. ABSTRACT *(Maximum 200 words)*

The compression strength of a stitched and a toughened matrix graphite/epoxy composite was determined and compared to a baseline unstitched untoughened composite. Two different layups with a variety of test lengths were tested under both ambient and hot/wet conditions. No significant difference in strength was seen for the different materials when the gage lengths of the specimens were long enough to lead to a buckling failure. For shorter specimens, a 30% reduction in strength from the baseline was seen due to stitching for both a 48-ply quasi-isotropic and a (0/45/0/-45/90/-45/0/45/0)s laminate. Analysis of the results suggested that the decrease in strength was due to increased fiber misalignment due to the stitches. An observed increasing strength with decreasing gage length, which was seen for all materials, was explained with a size effect model. The model assumed a random distribution of flaws (misaligned fibers). The toughened materials showed a small increase in strength over the baseline material both laminates presumably due to the compensating effects of a more compliant matrix and straighter fibers in the toughened material. The hot/wet strength of the stitched and baseline material fell 30% below their ambient strengths for shorter, non-buckling specimen, while the strength of the toughened matrix material only fell 20%. Video images of the failing specimen were recorded and showed local failures prior to global collapse of the specimen. These images support the theory of a random distribution of flaws controlling composite failure. Failed specimen appearance however, seems to be a misleading indication of the cause of failure.

14. SUBJECT TERMS
Composite material; Carbon epoxy; Stitched laminates; Toughened epoxy; Fiber misalignment

15. NUMBER OF PAGES
45

16. PRICE CODE
A03

17. SECURITY CLASSIFICATION OF REPORT	18. SECURITY CLASSIFICATION OF THIS PAGE	19. SECURITY CLASSIFICATION OF ABSTRACT	20. LIMITATION OF ABSTRACT
Unclassified	Unclassified		

NSN 7540-01-280-5500

Standard Form 298 (Rev. 2-89)
Prescribed by ANSI Std. Z39-18
298-102